Published in final edited form as:
Water Res. 2019 July 01; 158: 136–145. doi:10.1016/j.watres.2019.04.014.

Dynamics of the Physiochemical and Community Structure of Biofilm under the Influence of Algal Organic Matter and Humic Substances

Lei Li[1], **Youchul Jeon**[1,†], **Sang-Hoon Lee**[1,†], **Hodon Ryu**[2], **Jorge W. Santo Domingo**[2], and **Youngwoo Seo**[1,3,*]

[1] Department of Civil and Environmental Engineering, University of Toledo, Mail Stop 307, 3048 Nitschke Hall, Toledo, OH, USA

[2] Water Systems Division, National Risk Management Research Laboratory, U.S. Environmental Protection Agency, Cincinnati, Ohio 45268, United States

[3] Department of Chemical Engineering, University of Toledo, Mail Stop 307, 3048 Nitschke Hall, Toledo, OH, USA

Abstract

Increased loading of algal organic matter (AOM) during harmful algal blooms not only burdens water treatment processes but also challenges safe drinking water delivery. While organic constituents promote biofilm growth in drinking water distribution systems (DWDS), the effects of AOM on biofilm formation in DWDS are not well understood. Herein, three parallel biofilm reactors were used to assess and compare how AOM and humic substance (HS)-impacted bulk water, and R2A medium (a control) affect biofilm development for 168 days. The 16S rRNA gene sequencing analyses revealed that the bacterial communities in biofilms were clustered with the organic matter types in bulk water, where Family *Comamonadaceae* was the most dominant but showed different temporal dynamics depending on the organic matter characteristics in bulk water. Higher diversity was observed in the biofilm grown in AOM-impacted bulk water (BFAOM) than biofilm grown in HS-impacted (BFHS) and R2A-impacted bulk water (BFR2A) as the biofilm matured. In addition, some taxa (e.g., *Rhodobacteraceae*, and *Sphingomonadaceae*) were enriched in BFAOM compared to BFHS and BFR2A. The biofilm image analysis results indicated that compared to BFHS, BFAOM and BFR2A had relatively thinner and heterogeneous physical structures with lower amounts of cell biomass, extracellular polymeric substances (EPS), and higher EPS protein/polysaccharide ratios. Overall, this study revealed that how differently AOM and HS-impacted bulk water shape the physiochemical and community structure of biofilm, which can provide insights into assessing biofilm-associated risks and optimizing disinfection practices for biofilm control in DWDS.

[*]Corresponding author's mailing address: 3006 Nitschke Hall, Mail Stop 307, 2801 W. Bancroft St., Toledo, OH 43606-3390; Phone: (419) 530-8131; Fax: (419) 530-8116; Youngwoo.Seo@utoledo.edu.
[†]These authors (alphabetical order) contributed equally to this work.

Keywords

Algal organic matter; Humic substance; Biofilm development; Physiochemical and community structure; Drinking water

1. Introduction

The frequent occurrence of harmful algal blooms (HABs) by cyanobacteria poses adverse effects to drinking water supplies worldwide (Pivokonsky et al. 2016, Zhou et al. 2015). Preoxidation (e.g., potassium permanganate, ozone, etc.) coupled with coagulation and sedimentation has been broadly used to address the suddenly increased load of algal cells and algal organic matter (AOM) during HAB outbreaks (Xie et al. 2013, Zhou et al. 2015). However, these physiochemical treatments can also result in the release of intracellular AOM from disrupted algal cells, which can additionally contribute to AOM pools (Ma et al. 2012). AOM contains a high fraction of hydrophilic and small molecular compounds that as a whole, are difficult to be completely removed by water treatment processes, even with an advanced treatment method like ozonation (Joh et al. 2011, Zhou et al. 2015). Thus, those unremoved AOM can still exist in the finished water and subsequently enter drinking water distribution systems (DWDS), causing taste and odor issues and the formation of toxic disinfection by-products (DBPs) (Pivokonsky et al. 2016). Furthermore, as organic substrates, AOM could promote the growth of microbial biofilms in oligotrophic DWDS (Hammes et al. 2007).

Controlling biofilm formation is one of the most difficult tasks for delivering microbially-stable drinking water. In DWDS, about 90% of bacteria tend to attach to the interior surface of pipes and form biofilm (Flemming et al. 2002). Biofilm is an assemblage of microbial cells embedded in self-produced extracellular polymeric substances (EPS), which are primarily composed of polysaccharides and proteins (Flemming et al. 2002). Biofilm characteristics are highly associated with critical issues in DWDS. It has been reported that the physical structure of biofilm affects biofilm inactivation (Xu et al. 2018, Xue et al. 2014) and initial adhesion of pathogens (e.g. *Escherichia coli*, and *Legionella pneumophila*) within biofilm (Janjaroen et al. 2013, Shen et al. 2015, Wu et al. 2012), impacting biofilm proliferation and the biofilm-mediated fate and transport of pathogens in DWDS. The biomolecular composition of biofilm (EPS composition) can impact disinfectant reactions and transports in biofilm matrices, subsequently influencing both biofilm disinfection (e.g., preferential reaction of monochloramine with protein components than polysaccharides in EPS) (Xue et al. 2014, Xue et al. 2012) and biofilm-derived DBP formation and speciation (Wang et al. 2013). Furthermore, studies also indicated that the microbial community structure of biofilm is strongly related to the disinfection efficacy since some key microorganisms play an important role in the resistance of biofilms against disinfectants (Bridier et al. 2011, Simoes et al. 2010). Therefore, an understanding of biofilm structure, specifically its physiochemical and microbial community compositions, is crucial for maintaining the biological stability in DWDS.

As the primary nutrient source, the characteristics of organic matter in bulk water are among the most critical factors associated with biofilm formation and development in DWDS (Camper 2004). However, considerably less information is available to understand the interactions between mixed-species biofilm and commonly-available complex nutrient mixtures in DWDS, being mostly limited to humic substances (HS) (Camper 2004). HS are a primary source of terrestrially-derived organic matter found in DWDS (Volk and LeChevallier 2000). It was reported that HS could be effectively utilized by biofilm, having biomass yields within the same order of magnitude with more easily biodegradable organic molecules (Camper 2004). On the other hand, besides HS, AOM is also another possible source of organic matter within DWDS, as many water utilities recently face great challenges in managing AOM. In contrast to HS, AOM includes more nitrogenous components, which consist mainly of amino acids, polysaccharides, lipids, and other small molecules (Zhou et al. 2015). However, to our best knowledge, no research has been conducted to study the impacts of AOM on biofilm growth. Furthermore, an in-depth understanding of how HS and AOM-impacted bulk water differently affect the physical, chemical, and microbial community structure in biofilm succession is also missing, although these biofilm properties are known to affect disinfectant efficacy and biofilm-associated risks in DWDS. Given the fact that biofilm is widely present in DWDS and significantly influences the safe drinking water production, a comprehensive understanding of how biofilms develop and respond to complex nutrient sources in DWDS is imperative.

Accordingly, this study aims to investigate the effects of treated AOM and HS-impacted bulk water in biofilm development under unchlorinated DWDS conditions. Biofilm reactors were used and operated for 168 days. The formation, development, physiochemical characteristics, and community structure of biofilms exposed to AOM, HS, or R2A medium (control) were continuously monitored and compared using a confocal laser-scanning microscope (CLSM) and 16S rRNA gene sequencing analyses.

2. Materials and methods

2.1 Experimental design and reactor operation

Biofilms were grown in Centers for Disease Control and Prevention (CDC) biofilm reactors (BioSurface Technologies, MT, USA; Fig. S1) to simulate biofilm formation in DWDS. The reactors were operated at room temperature (24 ± 2 °C) under dark conditions (Revetta et al. 2016). Each reactor contained 24 removable PVC coupons and biofilms were grown in both sides of coupons (growth area: 1.25 × 2 cm^2). The cylinder rotation speed of all the reactors was set at 100 rpm to simulate the shear stress exerted on pipe surfaces in DWDS (30.5 cm/sec flow through 10.2 cm pipes). A disinfectant was not applied to the reactors, considering biofilm development under very low or no disinfectant residuals found at different locations in DWDS and premise plumbing (Abokifa et al. 2016, Proctor et al. 2016).

Initially, mixed-species bacterial inoculum (2×10^5 CFU/mL) were collected from local water utilities (filter effluents and DWDS) and inoculated into three parallel CDC reactors. The AOM stock solutions were prepared using cyanobacteria-laden water samples from Lake Erie according to the USEPA Method 545. HS stock solutions were prepared using a

commercial product (Sigma Aldrich, MO, USA). A granular-activated carbon filter (GAC; Calgon Carbon, PA, USA) was applied to remove residual disinfectants, DBPs, and the remaining total organic carbon (TOC) in tap water. After GAC filtration, the filtered tap water was used to dilute the AOM or HS stock solutions and treated by coagulation, flocculation, sedimentation, and ozonation to obtain the final TOC concentrations of 1.5 mg/L. Ozonation was added to the conventional treatment train as many water utilities affected by HABs already installed or are planning to install ozone to handle AOM. Granular filtration was not used after ozonation to eliminate other uncertainties (e.g., bacteria growth/releases and soluble microbial products (SMP) from filters) and maintain similar treated water quality. More details for the preparation of HS or AOM-impacted bulk waters are described in Text S1. Prepared HS and AOM-impacted bulk waters (reactor influent) were stored in sealed tanks with air filters and were directly delivered to HS or AOM reactors using a multichannel peristaltic pump (Cole-Parmer, IL, USA). The flow rate was 0.5 mL/min and the hydraulic retention time was twelve hour. For comparison, ologotrophic R2A medium (Teknova, CA, USA), which is normally used to enumerate bacteria in drinking water (Reasoner and Geldreich 1985), was used as a control. Sterilized R2A stock solution was directly injected to the R2A reactor using a syringe pump (KD Scientific, MA, USA) to prevent any potential contaminations. Meanwhile, for diluting the R2A stock solution, the ozonated tap water (after GAC filtration) was also delivered to the R2A reactor using a peristaltic pump. The final TOC concentration within this reactor was also maintained at around 1.5 mg/L. The TOC level was selected because it is the common TOC concentration found in many DWDS in the United States (Baribeau 2006). At this particular TOC level, the assimilable organic carbon (AOC) concentrations of HS, AOM, and R2A impacted-bulk water were 137.27 ± 9.29, 139.27 ± 12.25 and 140.37 ± 16.23 μg/L, respectively, which were within the range of common AOC values (18 to 214 μg/L) in DWDS (Volk and LeChevallier 2000). For this study, biofilms grown in different reactors which supplemented with HS, AOM, and R2A are identified as BFHS, BFAOM, and BFR2A, respectively.

2.2 Water chemistry and organic matter composition of bulk water

During reactor operations, turbidity, pH, TOC, total nitrogen (TN), and phosphate (PO_4^{3-}) of bulk water were monitored. Additionally, AOC was measured accordingly to a previously established method and the specific UV absorbance at 254 nm ($SUVA_{254}$) was recorded to compare the aromatic carbon contents in different bulk waters (Hammes et al. 2007, Weishaar et al. 2003). Fluorescence excitation-emission matrix (EEM) spectroscopy coupled with parallel factor analysis (PARAFAC) was applied to characterize the organic matter composition in bulk water. Additional details of the relevant analyses are provided in Text S2.

2.3 Biofilm physiochemical structure analyses

Three biofilm-grown coupons were taken out from each reactor every 21 days for 168 days and the clean coupons were installed again to provide the same surface area for biofilm to grow. For biofilm imaging, at least eight locations in a coupon were randomly selected for image acquisitions. Additional details of the biofilm staining and CLSM settings are provided in Text S3. The collected CLSM images were further analyzed using the

COMSTAT program (Heydorn et al. 2000) to determine biofilm parameters: (1) cell biomass (cell biovolume), (2) average thickness, (3) roughness coefficient, (4) surface area to volume ratio, (5) total EPS, and (6) protein/polysaccharide ratio. The roughness coefficient (R_a^*) can be calculated by the following equation according to Heydorn et al. (2000):

$$R_a^* = \frac{1}{N}\sum_{i=1}^{N}\frac{L_{fi} - \bar{L}_f}{\bar{L}_f} \quad (1)$$

Where L_{fi} = the ith individual thickness measurement, $\bar{L}_f$ = the mean thickness, and N = the number of thickness measurements.

2.4 Bacterial community analyses

2.4.1 Sample collection, DNA extraction, and high-throughput sequencing—

For bacterial community analyses, two collected coupons from each reactor were transferred to 50 mL Falcon tubes and resuspended in 10 mL sterile phosphate-buffered saline. Biofilms were detached from the coupons using mechanical scraping coupled with high-speed vortexing for 15 minutes and then mixed by a tissue-homogenizer. To have sufficient biomass, the homogenized biofilm solutions from two coupons were mixed together and centrifuged at 10,000 × g for 10 min. After discarding the supernatant, the pellets were collected and used for DNA extractions according to the manufacturer's instructions (PowerSoil DNA isolation kits; MoBio, CA, USA). Bacterial 16S rRNA genes were amplified from the DNA extracts of 24 biofilm samples and 1 initial inoculum using 515F and 806R bacterial universal primers (Caporaso et al. 2012). The Illumina Miseq and PE250 kits were used to generate the metabarcoded sequence libraries detailed elsewhere (Kapoor et al. 2016). Bulk water (influent) samples were not processed for molecular analyses as no colonies were detected in the heterotrophic media plates for ozonated bulk water stored in sealed influent tanks (Xu et al. 2002).

2.4.2 Sequencing data analyses—

The 16S rRNA gene sequence libraries were analyzed using the Quantitative Insights Into Microbial Ecology (QIIME) program (version 1.91) (Caporaso et al. 2010). Briefly, the paired-end sequence reads were trimmed and merged using the USEARCH 10 (Edgar 2010). An open-reference Operational Taxonomic Unit (OTU) picking method was applied in QIIME at similarity cutoff of 97% using Greengenes 16S rRNA gene database v13_8. After removing singleton OTUs (the OTUs appeared only once across the full OTU table), the sequencing depth of the 21 samples ranged from 52,276 to 16,902. All samples were subsequently rarefied to the smallest sequencing depth of 16,902, which translated into 13,144 OTUs in total before other downstream analyses. Alpha diversity indices and beta diversity were calculated by using QIIME. Compute_core_microbiome.py in QIIME was applied to determine the core OTUs among sampling groups. The core OTU is often defined as the shared OTUs above a certain threshold (the threshold value was set at 100% in this study which means OTUs appeared in all samples) within defined categories (Shade and Handelsman 2012). The core OTUs were further categorized into three groups: (1) Universal core, shared among all biofilm samples

from three categories of bulk water; (2) Transient core, shared between all biofilm samples from two categories of bulk water (e.g., shared between BFHS and BFAOM); (3) Unique core, shared among all the biofilm samples within a specific bulk water category but excluded the universal and transient core. The remaining OTUs are termed as peripheral OTUs.

2.5 Statistical analyses

Shapiro-Wilks normality test was conducted for water chemistry parameters, biofilm physiochemical structure parameters, and sequencing data. The Students' t-test (2-tail) or non-parametric Mann-Whitney U test was subsequently performed to determine statistical differences between samples. Principal coordinate analysis (PCoA), analysis of similarity (ANOSIM) test, and similarity percentage analysis (SIMPER) were also used to further characterize the sequencing data. Non-parametric Spearman's rank correlation analysis was applied to explore the correlations between structural parameters of biofilm. More details are described in Text S4.

3. Results

3.1 Chemical characteristics of bulk water

Table 1 shows water quality analysis results for different bulk waters. pH, PO_4^{3-}, AOC and TOC were similar. The highest turbidity, $SUVA_{254}$, and TOC/TN ratio were found in the HS-impacted bulk water, while higher TN levels were observed in the AOM (TN = 2.08 ± 0.11) and R2A-impacted water (TN = 2.51 ± 0.22). In addition, five EEM-PARAFAC components (tyrosine-like materials, SMP-like materials, tryptophan-like materials, low molecular weight (LMW) humic-like substances and high molecular weight (HMW) humic-like substances) were identified to characterize the organic matter composition of bulk water (Fig. S2 & Table S1). Both tyrosine and tryptophan-like materials are mixtures of aromatic proteins (Chen et al. 2003). SMP-like materials are also mixtures of proteins associated with biological processes (Ni et al. 2011). Compared to LMW humic-like substances, HMW humic-like substances are commonly terrestrial-derived (Fellman et al. 2010). The five detected EEM-PARAFAC components were clustered tightly according to the bulk water categories (principal component analysis), which demonstrated the differences of organic matter composition in HS, AOM, and R2A-impacted bulk water (Fig. S3). As expected, HS-impacted bulk water was characterized by the highest amount of humic-like substances, which again (besides $SUVA_{254}$ values) indicated that it contained higher aromatic carbon fractions compared to AOM and R2A-impacted bulk water (Weishaar et al. 2003). Moreover, AOM-impacted bulk water was also dominated by humic-like substances but possessed higher proportions of SMP and tryptophan-like materials than HS-impacted bulk water. For R2A-impacted bulk water, tyrosine, tryptophan, and SMP-like materials were the most abundant.

3.2 Physiochemical structure of biofilm

3.2.1 Physical structural parameters of biofilm—After 21 days, there was no difference in cell biomass among BFHS, BFAOM, and BFR2A. However, more cell biomass was found in BFHS than those of the other two types of biofilms from day 42 on ($P < 0.05$,

Fig. 1A). On the other hand, BFAOM had larger amounts of cell biomass than those of BFR2A from day 105 on ($P < 0.05$, Fig. 1A). The cell biomass for BFHS, BFAOM, and BFR2A at the end of the study was 7.69 ± 0.40 ($\mu m^3/\mu m^2$), 4.13 ± 0.47 ($\mu m^3/\mu m^2$), and 3.48 ± 0.34 ($\mu m^3/\mu m^2$), respectively.

The average thickness of BFHS gradually increased, reaching 20.47 ± 2.13 μm after 168 days, which was significantly higher than those of BFAOM (11.00 ± 1.42μm) and BFR2A (10.19 ± 0.84 μm), respectively ($P < 0.01$, Fig. 1B). BFAOM and BFR2A showed significantly lower average thickness than BFHS from day 42 on ($P < 0.05$, Fig. 1B). However, there were no significant differences between BFAOM and BFR2A during the entire study and the average thickness of BFAOM and BFR2A seemed to reach a steady state after 126 days, ranging from 10.64 ± 1.26 μm to 11.00 ± 1.15 μm and from 9.65 ± 1.19 μm to 10.19 ± 0.84 μm, respectively.

Roughness coefficient is a physical structural parameter of biofilm describing how biofilm thickness varies. Lower roughness coefficients indicate a more homogeneous biofilm surface. During the operations, the roughness coefficients of biofilms decreased over time, where the roughness coefficients of BFHS were statistically lower than BFAOM and BFR2A at day 21 and from day 126 to 168 ($P < 0.05$, Fig. 1C). In addition, the roughness coefficients of BFAOM were significantly lower than BFR2A during the same period ($P < 0.05$, Fig. 1C).

Surface area to volume ratio reflects how much of biofilm is exposed to the bulk flows. The surface area to volume ratios of BFHS were significantly lower than those of BFAOM and BFR2A from day 126 on ($P < 0.05$, Fig. 1D). This result may be due to the higher cell biomass accumulation in BFHS, which reduced the void area between adjacent cells. However, no significant differences in surface area to volume ratio were observed for BFAOM and BFR2A during the entire study ($P > 0.05$, Fig. 1D).

3.2.2 EPS accumulation and chemical composition—

During the early stages of biofilm development (up to 42 days), there were no significant differences in total EPS accumulation among BFHS, BFAOM, and BFR2A ($P > 0.05$, Fig. 2A). The total EPS for BFHS were higher than those of BFAOM and BFR2A from day 63 on ($P < 0.05$, Fig. 2A). However, there were no significant differences in total EPS between BFAOM and BFR2A throughout the entire study ($P < 0.05$, Fig. 2A). The protein/polysaccharide ratio of EPS formed by BFAOM and BFR2A increased continuously after 21 days (Fig. 2B). The protein/polysaccharide ratio in EPS of BFR2A was significantly higher than BFAOM after 126 days ($P < 0.05$, Fig. 2B), while the ratio of EPS produced by BFHS was mostly constant during the entire study, ranging from 1.07 ~1.31.

3.3 Bacterial community analysis

3.3.1 Temporal variation in diversity—

Three diversity indices: richness, Faith's phylogenetic diversity (PD), and Pielou's evenness (PE), were selected to compare the alpha diversity of biofilm communities (Fig. 3). A decrease in PE for BFHS and PD for BFR2A was observed at day 63 and 105, respectively but started to recover after that. Increasing trends were also observed for the richness and PD of BFAOM from day 105 to 168. These

results were consistent with previous findings that bacterial communities of biofilms tend to become diverse towards a more mature status, although temporary reductions of diversity could happen at the initial development stage possibly due to certain species outcompeting others (Douterelo et al. 2018). Finally, higher diversity (richness, PD) and PE were noted for BFAOM than BFHS and BFR2A from day 126 to 168.

PCoA based on the weighted UniFrac distance matrix was selected to evaluate the dissimilarities among the bacterial communities of inoculum, BFHS, BFAOM, and BFR2A since it provided the highest explanatory values (Fig. 4). The ANOSIM test ($R = 0.59$, $P < 0.001$) further confirmed that samples from inoculum, BFHS, BFAOM, and BFR2A formed distinctive clusters. Except for the pH, PO_4^{3-}, AOC, TOC, and TOC/TN ratio, other bulk water characteristics showed significant influences in shaping bacterial community structures of biofilms, especially for the organic matter composition (Table S2). PCoA1 was mainly correlated to HMW humic-like substances ($R^2 = 0.54$, $P < 0.01$), while PCoA2 was strongly associated with tyrosine-like materials ($R^2 = 0.82$, $P < 0.001$), followed by SMP-like materials ($R^2 = 0.81$, $P < 0.001$).

3.3.2 Taxonomic profiling—Overall, the relative abundance of individual taxa highly varied over time for different samples (Fig. 5 & 6). At phylum level, *Proteobacteria* (92.52% −57.53%), *Actinobacteria* (9.62%−0.52%), *Bacteroidetes* (34.43%−0.74%), and *Acidobacteria* (11.12%−0.33%) were dominant in biofilm samples and inoculum (Fig. 5A). Within the *Proteobacteria*, *Gammaproteobacteria* (42.02%) was the most abundant in the inoculum, while in the BFHS samples, *Betaproteobacteria* predominated from day 84 to 168, maintaining an average abundance of 67.13 ± 3.42% (Fig. 5B). In BFAOM, *Betaproteobacteria* was highly abundant on day 21 (67.32%) but decreased to 23.32% by day 168, while the relative abundance of *Alphaproteobacteria* increased from 12.73% to 36.42% during the same period. Conversely, in BFR2A the initially abundant *Alphaproteobacteria* decreased over time, while *Betaproteobacteria* increased to an average of 50.23 ± 5.46% between day 126 and 168.

At the family level, *Pseudomonadaceae* was the most dominant (25.30%) in the original inoculum while *Comamonadaceae* was consistently abundant after 21 days across all the biofilm samples (Fig. 6). Members of this group belong to the major taxa affiliated to the universal core of all biofilms (see Material and Methods section for definition; Table S3) and explained the largest differences of bacterial communities (16.47% out of 80.97%) among BFHS, BFAOM, and BFR2A (Table S4). Besides *Comamonadaceae*, other dominant families also occurred but showed differences among biofilm samples. For example, in BFHS, *Pseudomonadaceae* and several unassigned families were predominant at different sampling days. In BFAOM, *Rhodobacteraceae* (5.50–12.51%), an unassigned family affiliated to order *Rhizobiales* (3.40–7.73%), and *Sphingomonadaceae* (2.72–11.31%) were dominant from day 84 to 168. In BFR2A, *Rhodobacteraceae* (26.25%) was dominant in day 21, but dominant families shifted after 63 days (e.g., *Rhodocyclaceae*, 4.45–23.5%; *Chitinophagaceae*, 4.24–13.24%; *Rhodospirillaceae*, 9.11–23.83%).

3.3.3 Core OTU analyses—Twelve universal cores (Fig. S4) were found in all biofilm samples, accounting for 31.9% of the total sequences. These universal cores (e.g., family

Comamonadaceae and *Rhodospirillaceae*, and genus *Methyloversatilis* and *Nitrospira*; Table S3) have also been found in other drinking water-related biofilms (e.g., DWDS and premise plumbing systems) (Ji et al. 2015, Ling et al. 2016). Fig. 7 shows the dynamics in the relative abundance of the universal core, transient core, unique core and peripheral OTUs. The proportions of universal core for BFHS were generally larger than BFAOM and BFR2A, which suggested that HS-impacted bulk water was more suitable to support the growth of ubiquitous bacteria. However, the proportions of unique core for both BFAOM and BFR2A were significantly higher than BFHS ($P < 0.05$). No significant differences were observed between BFAOM and BFR2A for the proportions of universal core ($P > 0.05$) as well as unique core ($P > 0.05$).

4. Discussion

4.1 Dynamics of biofilm communities under the effects of different bulk water

Although the relative abundance of most individual taxa strongly varied over time throughout the entire study (except for BFHS from day 126 on), family *Comamonadaceae* was the most abundant taxa in all biofilm samples (Fig. 5 & 6). Members of *Comamonadaceae* have been found in a broad range of DWDS conditions (e.g., low temperature, fast-flowing, and oligotrophic) (Ling et al. 2016, Proctor et al. 2016). It was also suggested that *Comamonadaceae* is vital to the initial cell adhesion, leading to the formation of biofilm (Di Gregorio et al. 2017). However, the temporal dynamics of *Comamonadaceae* varied among biofilm groups in this study. In BFHS, the relative abundance of *Comamonadaceae* increased from 33.82% (day 21) to 65.62 ± 2.85% (day 126 to 168), while in BFAOM, *Comamonadaceae* decreased from 66.13% (day 21) to 17.95% (day 168). The higher amounts of available aromatic carbon compounds in HS compared to AOM or R2A-impact bulk (Table 1) can be a possible reason to explain the consistent enrichment of *Commaonadaceae* in BFHS because members belonging to this family are well-known to utilize aromatic carbons for their growth (Vinas et al. 2005). Besides *Comamonadaceae*, other prevalent taxa also appeared but behaved differently among bulk water categories (Fig. 6). Since all the reactors were operated under the same conditions, except for the feed solutions (reactor influents), the different temporal dynamic patterns and the presence of feed solution-specific dominant taxa suggested that the organic matter composition of bulk water influenced the bacterial community of biofilm. The continuous accumulation of members of phylum *Armatimonadetes* and family *Rhodobacteraceae* over time was observed in BFAOM, but not in BFHS and BFR2A. *Armatimonadetes* is a group of Gram-negative bacteria. Thus far, no information is available to describe the interaction between *Armatimonadetes* and AOM. *Rhodobacteraceae*-related members are known as the primary colonizers of surfaces that promote initial biofilm formation (Elifantz et al. 2013). More importantly, *Rhodobacteraceae* was able to grow together with algae by utilizing the algal exudates such as glycolate, taurine, and polyamines (Williams et al. 2013). It was also reported that *Rhodobacteraceae* was the most abundant taxa associated with phytoplankton blooms (Buchan et al. 2005). Thus, it is not surprising that *Rhodobacteraceae*, which were dominant in BFR2A (26.24%) on day 21, quickly became rare, most likely due to a lack of appropriate nutrients or interspecies interactions. However, the relative abundance of *Rhodobacteraceae* gradually increased and the group became the second most dominant

family in BFAOM from day 147 on, followed by *Comamonadaceae*. In addition, phylum *Planctomycetes* (0.64–4.43%) and family *Sphingomonadaceae* (2.60%~11.32%) were also predominant and displayed significantly higher relative abundance in BFAOM, compared to BFHS and BFR2A ($P < 0.05$). *Planctomycetes* could degrade algal-derived compounds (Erbilgin et al. 2014, Jeske et al. 2013), while *Sphingomonadaceae* was found to be one of the most dominant taxa in biofilms of photobioreactors with microalgae (Krohn-Molt et al. 2013). Accordingly, these results again reinforced that the organic matter composition in bulk water is a strong external factor capable of impacting the composition of biofilm communities in DWDS.

Several full-scale DWDS studies reported that seasonality is the key contributor to shape biofilm community structures, where the authors proposed that the variation of seasonal water temperature was the major factor (Ling et al. 2016, Potgieter et al. 2018). When we consider the observations in this study (Fig. 4), the fluctuations in natural organic matter (NOM) composition in different seasons may be another factor that plays a role in the seasonal variations of biofilm communities in DWDS. It was reported that allochthonous NOM (e.g., HS) enters freshwater systems during the spring runoff, while autochthonous NOM (e.g., AOM) is mainly produced in the summer and early fall (Crump et al. 2003). Applying the same water treatment processes, the removal efficiency of different NOM may not be the same, which can subsequently result in different fractions of organic matter entering DWDS. Therefore, the variation of NOM composition in DWDS could affect biofilm communities in different seasons. In agreement with our speculations, Crump et al. (2003) indicated that seasonal shifts of microbial communities in lakes were related to changes in organic matter types (e.g., terrestrial versus phytoplankton). Another study also reported that the community structures of bacterial biofilm were shaped by source water characteristics within metropolitan DWDS (Revetta et al. 2016).

4.2 Dynamics of biofilm physicochemical structures under the influence of different bulk water

To understand the changes in the physicochemical structure of biofilm under the influence of different bulk water, CLSM image analyses were conducted. Overall, the most differences were observed between BFHS and BFAOM (or BFR2A). Highest cell biomass was accumulated in BFHS compared to BFAOM and BFR2A from day 42 on (Fig. 1A). A recent study revealed that the trends for the cell biomass quantity in different biofilms were correlated to whether available nutrients support the development of the universal bacterial core or not; higher cell biomass productions were observed in the biofilm containing higher proportions of the universal core (Proctor et al. 2016). The universal core usually represents the bacteria with fast growth and high colonization rates, stress tolerance, and overall adaptation, thus, leading to the formation of more cell biomass (Ji et al. 2015, Martiny et al. 2006, Proctor et al. 2016). In this study, similar trends were found in BFHS, which had a larger proportion of universal core than BFAOM and BFR2A, accordingly, possessing more cell biomass (Fig. 1A & Fig. 7).

Apart from the differences in cell biomass, the amounts of total EPS also varied among biofilm samples (Fig. 2A). At the given points, higher amounts of total EPS were observed

in BFHS, which contained higher cell biomass than BFAOM and BFR2A. Correlation analyses results indicated that their cell biomass and the amounts of total EPS were all positively correlated (Spearman rank correlation, Spearman's rank correlation coefficient (ρ) = 0.96 for BFHS, $\rho = 0.94$ for BFAOM, and $\rho = 0.88$ for BFR2A, $P < 0.05$), which potentially can imply that more cell biomass results in higher amounts of total EPS accumulation in biofilms. Moreover, in terms of the bacterial communities, as discussed before, although *Comamonadaceae* was the most dominant family in all biofilm samples, its relative abundance only showed an increasing trend in BFHS (up to 68.86% in day 168) but not in BFAOM and BFR2A. In addition to being important initial colonizers in biofilm, members belonging to family *Comamonadaceae* are known to produce large amounts of EPS (Gao et al. 2013, Subramanian et al. 2010). Therefore, it can be inferred that the higher total EPS contents in BFHS may also be closely associated with the continuous predominance and increased presence of *Comamonadaceae* in BFHS.

To closely examine the chemical composition of biofilm EPS, the protein/polysaccharide ratios were calculated (Fig. 2B). The proportions of protein to polysaccharide in BFHS ranged from 1 to 1.3, which were similar to previously-reported ratios (0.92~1.2) for biofilm grown in undisinfected DWDS (Shen et al. 2016). On the other hand, the protein/polysaccharide ratios in BFAOM and BFR2A increased over time and reached to 2.19 ± 0.10 and 2.52 ± 0.24, respectively, at day 168. It has been reported that the chemical composition of bacterial EPS depends on the C and N content of feeding substrates, of which protein production of EPS can be promoted when C/N ratios were low (Durmaz and Sanin 2001, Heldal et al. 1996). Thus, the results with higher protein/polysaccharide ratios in BFAOM and BFR2A than BFHS can be explained by the higher TN levels observed in AOM and R2A-impacted bulk water (Table 1). Besides the direct effects posed by the nutrient composition in bulk water, the differences in EPS chemical composition can also be explained by the distinctive bacterial community composition among BFHS, BFAOM, and BFR2A (Fig. 4). Generally, via various biosynthesis pathways, bacterial species even at the same genus level can produce different types of EPS (e.g., protein-based or polysaccharide-based) (Schmid et al. 2015, Xue et al. 2014). While 16S rRNA gene sequencing provided the bacterial composition of biofilm, further studies are needed using other advanced techniques (e.g., proteomics, metagenomics, and transcriptomics) to fully map the EPS synthesis pathway of individual taxa and correlate with the chemical compositions of EPS in these complex biofilm communities (Mason et al. 2012, Valenzuela et al. 2006).

In addition to the differences in biofilm EPS characteristics, other structural parameters of BFHS, BFAOM, and BFR2A were distinctively different (Fig. 1). Overall, BFHS showed a tendency to form thick, compact, and homogenous physical structures of biofilm over time, while BFAOM and BFR2A showed thinner and relatively heterogeneous physical structures. These observations were supported by the biofilm images, where BFAOM and BFR2A had more porous biofilm structures with large channels and voids, particularly in BFR2A (Fig. S5). The correlation analysis results showed that the roughness coefficients of BFHS, BFAOM, and BFR2A correlated well with their EPS protein/polysaccharide ratios (Spearman rank correlation, $\rho = 0.75$ for BFHS, $\rho = -0.98$ for BFAOM, and $\rho = -0.99$ for BFR2A, $P < 0.05$). The values of Spearman's rank correlation coefficient (closed to −1 or 1) indicated that the physical properties of biofilm are strongly associated with its EPS protein/

polysaccharide ratios. Moreover, when the biofilm became mature (from day 126 to 168), at given points, the biofilm EPS (BFAOM and BFR2A), which contained higher protein proportions, tended to have higher heterogeneity (Fig. 1C & Fig. 2B). In other words, BFHS, which possessed higher EPS polysaccharide proportions compared to BFAOM and BFR2A, had relatively homogeneous physical structures. These observed patterns could be explained by the close-ranged electrostatic interactions among the functional groups of polysaccharides, which are known to enhance the “bridging effects”, therefore resulting in the formation of more homogenous physical structures of BFHS (Desmond et al. 2018).

In summary, the data indicates that there is a complex “interaction web” among the organic matter characteristics in bulk water, bacterial community composition of biofilm and its physiochemical structures. Specifically, organic matter can cause direct impacts on biofilm development. More importantly, the responded bacterial communities can also affect the EPS production and chemical composition of the entire biofilm matrix, therefore, eventually leading to the development of biofilms with unique structures. To better elucidate the mechanisms behind this “interaction web”, future research is needed to understand the individual or cross-link metabolomic profiling of biofilm in response to the different organic matter.

4.3 Practical implications

The DWDS management requires a comprehensive understanding of many aspects of water supply and distribution as well as water chemistry and microbiology. Biofilm is ubiquitous in DWDS, especially in locations with very low or no disinfectant residuals due to the high-water age, the presence of disinfectant demanding substances, or prolonged water stagnation. If there are biofilm and/or pathogen outbreaks like the Legionnaires’ disease outbreak in DWDS during the Flint water crisis in the United States, the common strategy for water utilities to control microbial contaminants is to increase the disinfectant dose to maintain disinfectant residuals throughout the DWDS. The results of this study on biofilm development under the influence of different drinking water-related organic matter can provide insights into managing and improving DWDS operations. Specifically, the direct impacts of organic matter on the physiochemical and bacterial community structures of biofilm suggest that: (1) compared to AOM, utilities treating HS-impacted source water may experience more biofilm formation with higher biofilm thickness, cell biomass, and total EPS, which may lead to fast disinfectant decay and high disinfectant demand in DWDS; (2) different disinfectant reaction, transport, and decay are expected in BFHS and BFAOM, as they hold different physical structures and biomolecular composition of biofilm, which can subsequently affect the biofilm disinfection efficacy and DBP formation and speciation from biofilm upon disinfectant exposure; (3) compared to BFHS, enhanced pathogen entrapment in BFAOM is expected, as it has distinctive physical structures with higher surface roughness, which increases initial adhesion of pathogens in biofilm matrices. Accordingly, understanding the organic matter characteristics of source water should be considered as an indispensable step to assess the biofilm-associated risk and develop biofilm disinfection strategies in DWDS operations. In the future, the impacts of other DWDS conditions on biofilm (e.g., pipe materials, temperature, disinfectant types, etc.) and biofilm interaction

with pathogens need to be further explored under long-term exposure to HS or AOM-impacted water.

5. Conclusions

This study examined the dynamic changes of biofilm in response to AOM, HS, and R2A-impacted bulk water at similar TOC/AOC levels for 168 days. The major findings were:

- The taxa, *Comamonadaceae,* associated with biofilm formation and EPS production, was the most dominant in all biofilm samples but showed different dynamic patterns, depending on the organic matter characteristics of bulk water. Besides *Comamonadaceae*, other taxa, phylum *Planctomycetes*, and family *Rhodobacteraceae* and *Sphingomonadaceae* were also enriched and predominated in BFAOM compared to BFHS and BFR2A. As biofilm matured, higher diversity with more relative abundance of unique core was observed in BFAOM than BFHS, which contained higher relative abundance of universal core.
- AOM and R2A-impacted-bulk water supported the growth of biofilm with relatively thinner and heterogeneous physical structures that contained less cell biomass and total EPS, but higher amounts of proteins than polysaccharides in their EPS contents. In contrast, HS-impacted bulk water supported the growth of biofilm with thicker and more homogeneous physical structures that contained higher cell biomass and total EPS, but lower amounts of proteins than polysaccharides in its EPS contents.
- Organic matter characteristics of source water should be considered as an essential factor to assess biofilm-associated risks and develop disinfection protocols for biofilm control in DWDS operations.

Supplementary Material

Refer to Web version on PubMed Central for supplementary material.

Acknowledgements

This study was supported by the National Science Foundation (CBET 1236433 & 1605185) and in part by the U.S. Environmental Protection Agency (USEPA). Any opinions expressed do not reflect the views of the agency; therefore, no official endorsement should be inferred. Any mention of trade names or commercial products does not constitute endorsement or recommendation for use. Authors also appreciate Dr. Dae-wook Kang for providing critical comments of the manuscript and Ms. Abigail Calmes, Samantha Heitzenrater, and Faith Seo for proofreading the manuscript.

Reference

Abokifa AA, Yang YJ, Lo CS and Biswas P (2016) Water quality modeling in the dead end sections of drinking water distribution networks. Water Research 89, 107–117. [PubMed: 26641015]

Baribeau H.l. (2006) Formation and decay of disinfection by-products in the distribution system, American Water Works Association.

Bridier A, Briandet R, Thomas V and Dubois-Brissonnet F (2011) Resistance of bacterial biofilms to disinfectants: a review. Biofouling 27(9), 1017–1032. [PubMed: 22011093]

Buchan A, González JM and Moran MA (2005) Overview of the marine Roseobacter lineage. Applied and Environmental Microbiology 71(10), 5665–5677. [PubMed: 16204474]

Camper AK (2004) Involvement of humic substances in regrowth. International Journal of Food Microbiology 92(3), 355–364. [PubMed: 15145594]

Caporaso JG, Kuczynski J, Stombaugh J, Bittinger K, Bushman FD, Costello EK, Fierer N, Pena AG, Goodrich JK and Gordon JI (2010) QIIME allows analysis of high-throughput community sequencing data. Nature methods 7(5), 335. [PubMed: 20383131]

Caporaso JG, Lauber CL, Walters WA, Berg-Lyons D, Huntley J, Fierer N, Owens SM, Betley J, Fraser L and Bauer M (2012) Ultra-high-throughput microbial community analysis on the Illumina HiSeq and MiSeq platforms. The ISME journal 6(8), 1621. [PubMed: 22402401]

Chen W, Westerhoff P, Leenheer JA and Booksh K (2003) Fluorescence excitation− emission matrix regional integration to quantify spectra for dissolved organic matter. Environmental science & technology 37(24), 5701–5710. [PubMed: 14717183]

Crump BC, Kling GW, Bahr M and Hobbie JE (2003) Bacterioplankton community shifts in an arctic lake correlate with seasonal changes in organic matter source. Applied and Environmental Microbiology 69(4), 2253–2268. [PubMed: 12676708]

Desmond P, Best JP, Morgenroth E and Derlon N (2018) Linking composition of extracellular polymeric substances (EPS) to the physical structure and hydraulic resistance of membrane biofilms. Water Research 132, 211–221. [PubMed: 29331909]

Di Gregorio L, Tandoi V, Congestri R, Rossetti S and Di Pippo F (2017) Unravelling the core microbiome of biofilms in cooling tower systems. Biofouling 33(10), 793–806. [PubMed: 28994320]

Douterelo I, Fish K and Boxall J (2018) Succession of bacterial and fungal communities within biofilms of a chlorinated drinking water distribution system. Water Research 141, 74–85. [PubMed: 29778067]

Durmaz B and Sanin F (2001) Effect of carbon to nitrogen ratio on the composition of microbial extracellular polymers in activated sludge. Water Science and Technology 44(10), 221–229.

Edgar RC (2010) Search and clustering orders of magnitude faster than BLAST. Bioinformatics 26(19), 2460–2461. [PubMed: 20709691]

Elifantz H, Horn G, Ayon M, Cohen Y and Minz D (2013) Rhodobacteraceae are the key members of the microbial community of the initial biofilm formed in Eastern Mediterranean coastal seawater. FEMS microbiology ecology 85(2), 348–357. [PubMed: 23551015]

Erbilgin O, McDonald KL and Kerfeld CA (2014) Characterization of a planctomycetal organelle: a novel bacterial microcompartment for the aerobic degradation of plant saccharides. Applied and Environmental Microbiology 80(7), 2193–2205. [PubMed: 24487526]

Fellman JB, Hood E and Spencer RG (2010) Fluorescence spectroscopy opens new windows into dissolved organic matter dynamics in freshwater ecosystems: A review. Limnology and Oceanography 55(6), 2452–2462.

Flemming H-C, Percival S and Walker J (2002) Contamination potential of biofilms in water distribution systems. Water science and technology: water supply 2(1), 271–280.

Gao D, Fu Y and Ren N (2013) Tracing biofouling to the structure of the microbial community and its metabolic products: A study of the three-stage MBR process. Water Research 47(17), 6680–6690. [PubMed: 24064549]

Hammes F, Meylan S, Salhi E, Köster O, Egli T and Von Gunten U (2007) Formation of assimilable organic carbon (AOC) and specific natural organic matter (NOM) fractions during ozonation of phytoplankton. Water Research 41(7), 1447–1454. [PubMed: 17321564]

Heldal M, Norland S, Fagerbakke KM, Thingstad F and Bratbak G (1996) The elemental composition of bacteria: a signature of growth conditions? Marine pollution bulletin 33(1–6), 3–9.

Heydorn A, Nielsen AT, Hentzer M, Sternberg C, Givskov M, Ersbøll BK and Molin S (2000) Quantification of biofilm structures by the novel computer program COMSTAT. Microbiology 146(10), 2395–2407. [PubMed: 11021916]

Janjaroen D, Ling F, Monroy G, Derlon N, Mogenroth E, Boppart SA, Liu W-T and Nguyen TH (2013) Roles of ionic strength and biofilm roughness on adhesion kinetics of Escherichia coli onto

groundwater biofilm grown on PVC surfaces. Water Research 47(7), 2531–2542. [PubMed: 23497979]

Jeske O, Jogler M, Petersen J, Sikorski J and Jogler C (2013) From genome mining to phenotypic microarrays: Planctomycetes as source for novel bioactive molecules. Antonie Van Leeuwenhoek 104(4), 551–567. [PubMed: 23982431]

Ji P, Parks J, Edwards MA and Pruden A (2015) Impact of water chemistry, pipe material and stagnation on the building plumbing microbiome. PLoS One 10(10), e0141087. [PubMed: 26495985]

Joh G, Choi YS, Shin J-K and Lee J (2011) Problematic algae in the sedimentation and filtration process of water treatment plants. Journal of Water Supply: Research and Technology-Aqua 60(4), 219–230.

Kapoor V, Elk M, Li X, Impellitteri CA and Santo Domingo JW (2016) Effects of Cr (III) and Cr (VI) on nitrification inhibition as determined by SOUR, function-specific gene expression and 16S rRNA sequence analysis of wastewater nitrifying enrichments. Chemosphere 147, 361–367. [PubMed: 26774300]

Krohn-Molt I, Wemheuer B, Alawi M, Poehlein A, Güllert S, Schmeisser C, Pommerening-Röser A, Grundhoff A, Daniel R and Hanelt D (2013) Metagenome survey of a multispecies and alga-associated biofilm revealed key elements of bacterial-algal interactions in photobioreactors. Applied and Environmental Microbiology 79(20), 6196–6206. [PubMed: 23913425]

Ling F, Hwang C, LeChevallier MW, Andersen GL and Liu W-T (2016) Core-satellite populations and seasonality of water meter biofilms in a metropolitan drinking water distribution system. The ISME journal 10(3), 582. [PubMed: 26251872]

Ma M, Liu R, Liu H, Qu J and Jefferson W (2012) Effects and mechanisms of pre-chlorination on Microcystis aeruginosa removal by alum coagulation: significance of the released intracellular organic matter. Separation and purification technology 86, 19–25.

Martiny JBH, Bohannan BJ, Brown JH, Colwell RK, Fuhrman JA, Green JL, Horner-Devine MC, Kane M, Krumins JA and Kuske CR (2006) Microbial biogeography: putting microorganisms on the map. Nature Reviews Microbiology 4(2), 102. [PubMed: 16415926]

Mason OU, Hazen TC, Borglin S, Chain PS, Dubinsky EA, Fortney JL, Han J, Holman H-YN, Hultman J and Lamendella R (2012) Metagenome, metatranscriptome and single-cell sequencing reveal microbial response to Deepwater Horizon oil spill. The ISME journal 6(9), 1715. [PubMed: 22717885]

Ni B-J, Rittmann BE and Yu H-Q (2011) Soluble microbial products and their implications in mixed culture biotechnology. Trends in biotechnology 29(9), 454–463. [PubMed: 21632131]

Pivokonsky M, Naceradska J, Kopecka I, Baresova M, Jefferson B, Li X and Henderson R (2016) The impact of algogenic organic matter on water treatment plant operation and water quality: a review. Critical Reviews in Environmental Science and Technology 46(4), 291–335.

Potgieter S, Pinto A, Sigudu M, Du Preez H, Ncube E and Venter S (2018) Long-term spatial and temporal microbial community dynamics in a large-scale drinking water distribution system with multiple disinfectant regimes. Water Research 139, 406–419. [PubMed: 29673939]

Proctor CR, Gächter M, Kötzsch S, Rölli F, Sigrist R, Walser J-C and Hammes F (2016) Biofilms in shower hoses–choice of pipe material influences bacterial growth and communities. Environmental Science: Water Research & Technology 2(4), 670–682.

Reasoner DJ and Geldreich E (1985) A new medium for the enumeration and subculture of bacteria from potable water. Applied and Environmental Microbiology 49(1), 1–7. [PubMed: 3883894]

Revetta R, Gomez-Alvarez V, Gerke T, Santo Domingo J and Ashbolt N (2016) Changes in bacterial composition of biofilm in a metropolitan drinking water distribution system. Journal of applied microbiology 121(1), 294–305. [PubMed: 27037969]

Schmid J, Sieber V and Rehm B (2015) Bacterial exopolysaccharides: biosynthesis pathways and engineering strategies. Frontiers in microbiology 6, 496. [PubMed: 26074894]

Shade A and Handelsman J (2012) Beyond the Venn diagram: the hunt for a core microbiome. Environmental microbiology 14(1), 4–12. [PubMed: 22004523]

Shen Y, Huang C, Monroy GL, Janjaroen D, Derlon N, Lin J, Espinosa-Marzal R, Morgenroth E, Boppart SA and Ashbolt NJ (2016) Response of simulated drinking water biofilm mechanical and

structural properties to long-term disinfectant exposure. Environmental science & technology 50(4), 1779–1787. [PubMed: 26756120]

Shen Y, Monroy GL, Derlon N, Janjaroen D, Huang C, Morgenroth E, Boppart SA, Ashbolt NJ, Liu W-T and Nguyen TH (2015) Role of biofilm roughness and hydrodynamic conditions in Legionella pneumophila adhesion to and detachment from simulated drinking water biofilms. Environmental science & technology 49(7), 4274–4282. [PubMed: 25699403]

Simoes LC, Simoes M and Vieira MJ (2010) Influence of the diversity of bacterial isolates from drinking water on resistance of biofilms to disinfection. Applied and Environmental Microbiology 76(19), 6673–6679. [PubMed: 20693444]

Subramanian SB, Yan S, Tyagi RD and Surampalli R (2010) Extracellular polymeric substances (EPS) producing bacterial strains of municipal wastewater sludge: isolation, molecular identification, EPS characterization and performance for sludge settling and dewatering. Water Research 44(7), 2253–2266. [PubMed: 20122709]

Valenzuela L, Chi A, Beard S, Orell A, Guiliani N, Shabanowitz J, Hunt DF and Jerez CA (2006) Genomics, metagenomics and proteomics in biomining microorganisms. Biotechnology advances 24(2), 197–211. [PubMed: 16288845]

Vinas M, Sabaté J, Espuny MJ and Solanas AM (2005) Bacterial community dynamics and polycyclic aromatic hydrocarbon degradation during bioremediation of heavily creosote-contaminated soil. Applied and Environmental Microbiology 71(11), 7008–7018. [PubMed: 16269736]

Volk CJ and LeChevallier MW (2000) Assessing biodegradable organic matter. Journal-American Water Works Association 92(5), 64–76.

Wang Z, Choi O and Seo Y (2013) Relative contribution of biomolecules in bacterial extracellular polymeric substances to disinfection byproduct formation. Environmental science & technology 47(17), 9764–9773. [PubMed: 23866010]

Weishaar JL, Aiken GR, Bergamaschi BA, Fram MS, Fujii R and Mopper K (2003) Evaluation of specific ultraviolet absorbance as an indicator of the chemical composition and reactivity of dissolved organic carbon. Environmental science & technology 37(20), 4702–4708. [PubMed: 14594381]

Williams TJ, Wilkins D, Long E, Evans F, DeMaere MZ, Raftery MJ and Cavicchioli R (2013) The role of planktonic Flavobacteria in processing algal organic matter in coastal East Antarctica revealed using metagenomics and metaproteomics. Environmental microbiology 15(5), 1302–1317. [PubMed: 23126454]

Wu M-Y, Sendamangalam V, Xue Z and Seo Y (2012) The influence of biofilm structure and total interaction energy on Escherichia coli retention by Pseudomonas aeruginosa biofilm. Biofouling 28(10), 1119–1128. [PubMed: 23075008]

Xie P, Ma J, Fang J, Guan Y, Yue S, Li X and Chen L (2013) Comparison of permanganate preoxidation and preozonation on algae containing water: cell integrity, characteristics, and chlorinated disinfection byproduct formation. Environmental science & technology 47(24), 14051–14061. [PubMed: 24237350]

Xu J, Huang C, Shi X, Dong S, Yuan B and Nguyen TH (2018) Role of drinking water biofilms on residual chlorine decay and trihalomethane formation: An experimental and modeling study. Science of the Total Environment 642, 516–525. [PubMed: 29908510]

Xu P, Janex M-L, Savoye P, Cockx A and Lazarova V (2002) Wastewater disinfection by ozone: main parameters for process design. Water Research 36(4), 1043–1055. [PubMed: 11848343]

Xue Z, Lee WH, Coburn KM and Seo Y (2014) Selective reactivity of monochloramine with extracellular matrix components affects the disinfection of biofilm and detached clusters. Environmental science & technology 48(7), 3832–3839. [PubMed: 24575887]

Xue Z, Sendamangalam VR, Gruden CL and Seo Y (2012) Multiple roles of extracellular polymeric substances on resistance of biofilm and detached clusters. Environmental science & technology 46(24), 13212–13219. [PubMed: 23167565]

Zhou S, Zhu S, Shao Y and Gao N (2015) Characteristics of C-, N-DBPs formation from algal organic matter: role of molecular weight fractions and impacts of pre-ozonation. Water Research 72, 381–390.(Shen et al. 2016) [PubMed: 25479708]

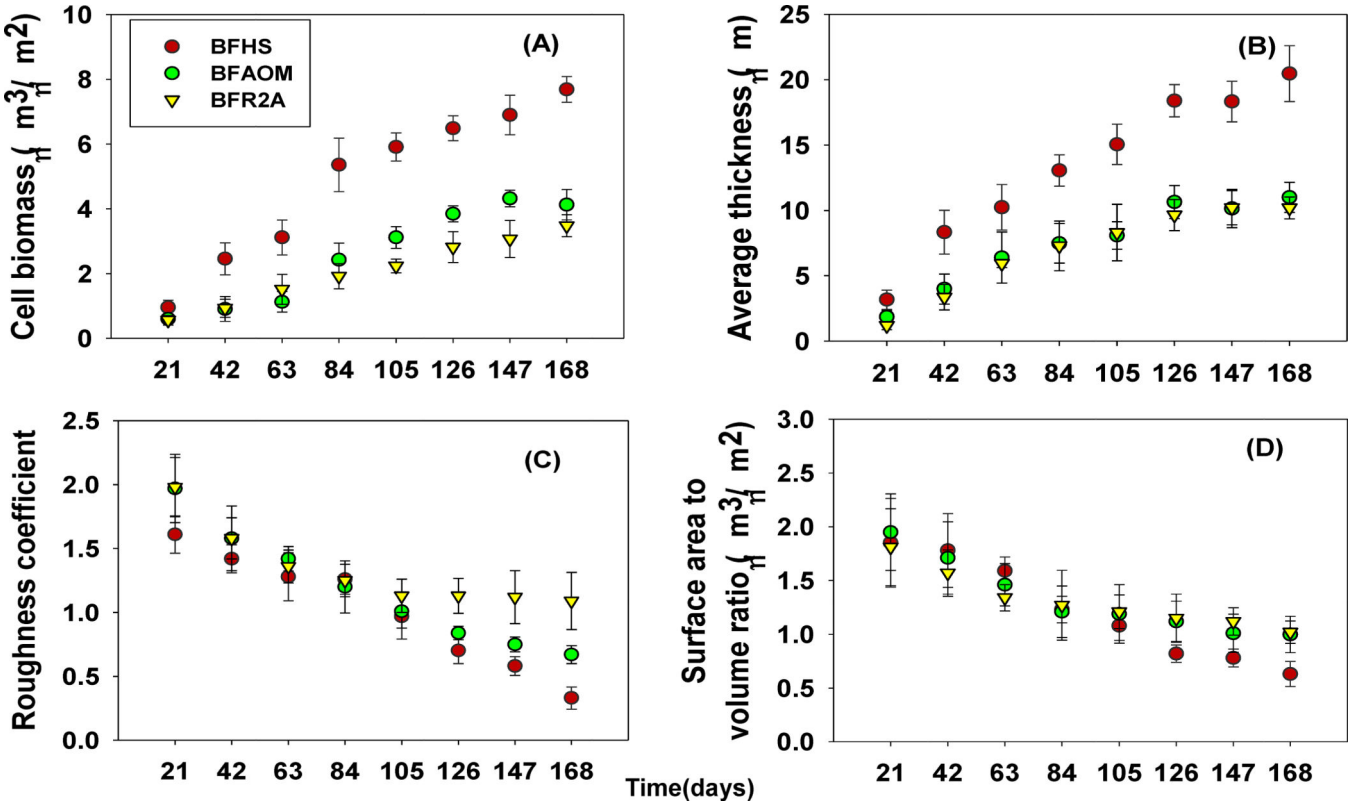

Fig. 1.

The dynamics of structural characteristics of biofilms (A) cell biomass, (B) average thickness, (C) roughness coefficient, and (D) surface area to volume ratio for 168 days of biofilm growth under HS-, AOM- and R2A-impacted bulk water. Minimum eight randomly selected locations in a coupon were imaged for each biofilm sample. Error bars indicate standard deviation among different locations ($n \geq 8$).

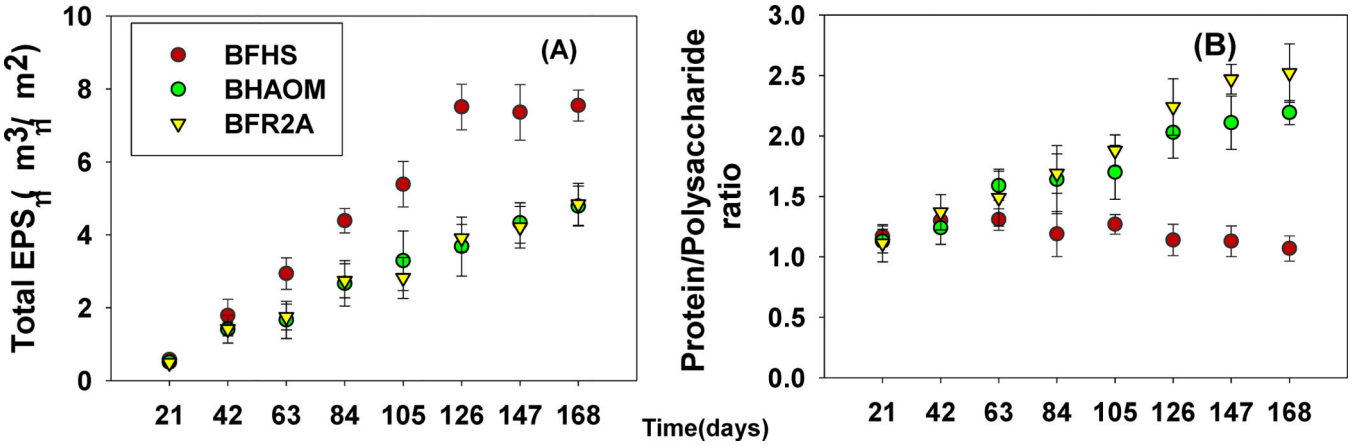

Fig. 2.

The dynamics of biofilm EPS formation (A) total EPS, and (B) protein/polysaccharide ratio for 168 days of biofilm growth under HS-, AOM-, and R2A-impacted bulk water. Minimum eight randomly selected locations in a coupon were imaged for each biofilm sample. Error bars indicate standard deviation among different locations ($n \geq 8$).

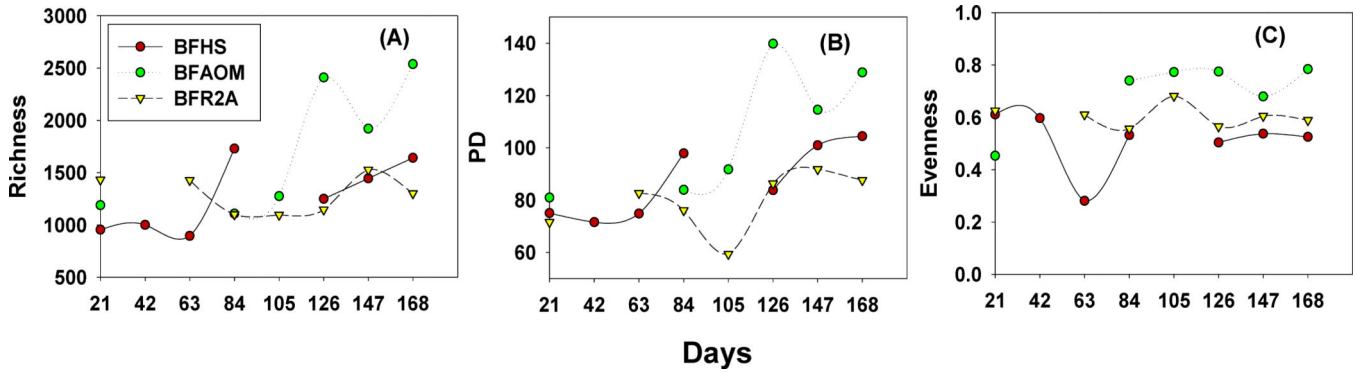

Fig. 3.

The dynamics of diversity indices for BFHS, BFAOM, and BFR2A samples: (A) Richness (total numbers of observed OTUs clustered at 97% sequence identity), (B) Faith's phylogenetic diversity (PD), and (C) Pielou's evenness (PE) for 168 days. For each biofilm sample, the DNA extracts from two biofilm grown-coupons were used for sequencing. The breakpoints correspond to lost samples.

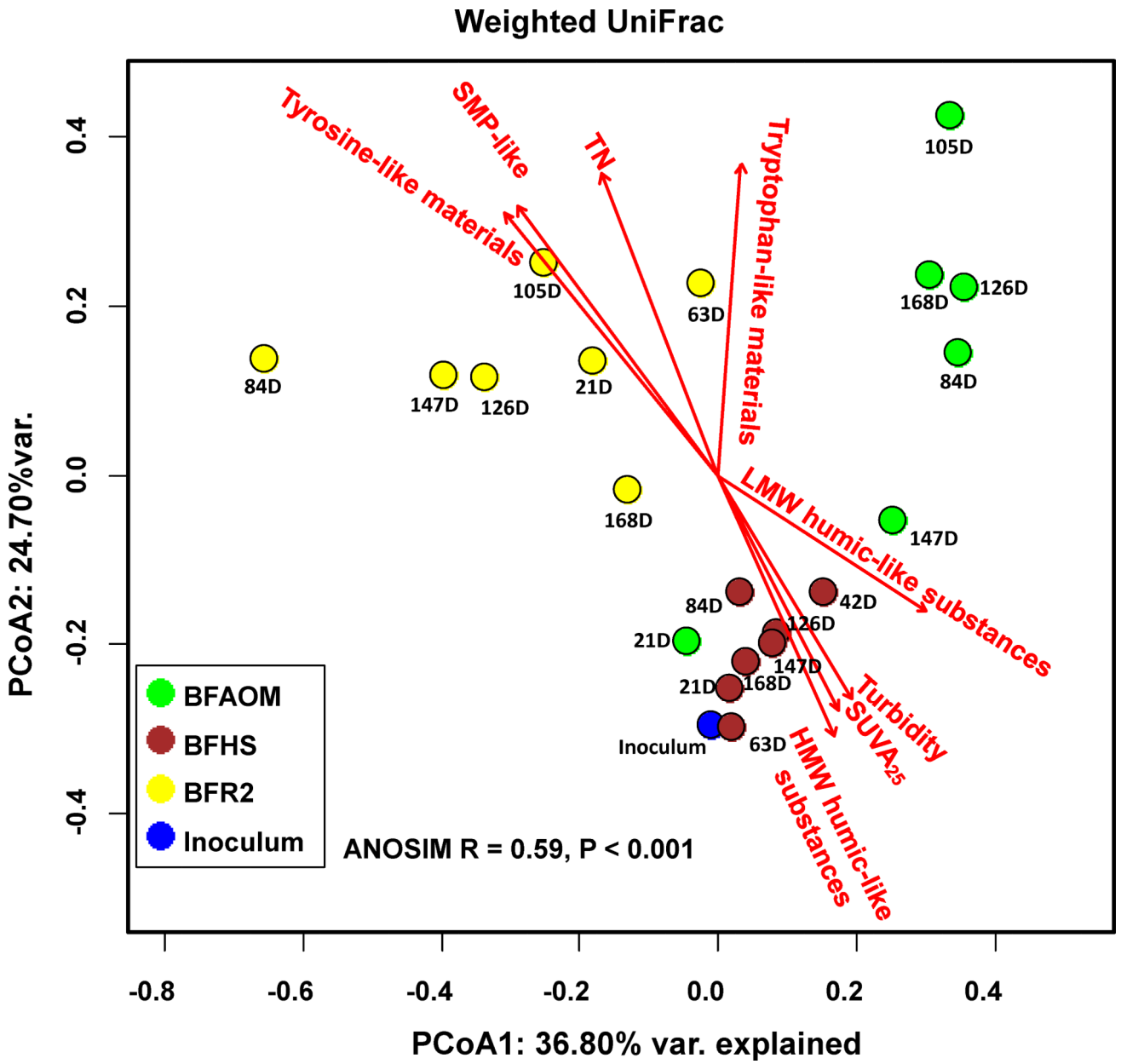

Fig. 4.

Principal coordinate analysis (PCoA) derived from the weighted UniFrac distance matrix of phylogenetic bacterial community structures. PCoA1 and PCoA2 explained 36.80% and 24.70% of the total variance, respectively. The strength of statistically significant ($P < 0.05$) explanatory variables is shown with solid red arrows. For each biofilm sample, the DNA extracts from two biofilm grown-coupons were used for sequencing.

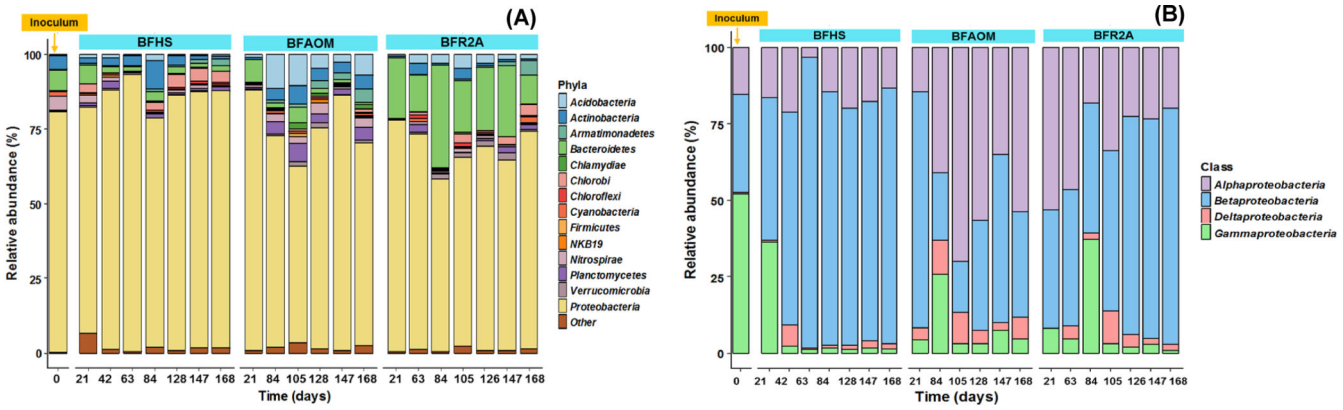

Fig. 5.

The dynamics of the bacterial community compositions in the inoculum, BFHS, BFAOM, and BFR2A samples: (A) relative abundance at the phylum level, (B) relative abundance at the class level affiliated to phylum *Proteobacteria*. "Other" represents taxa with relative abundance less than 1% in all samples and unassigned taxa. For each biofilm sample, the DNA extracts from two biofilm grown-coupons were used for sequencing.

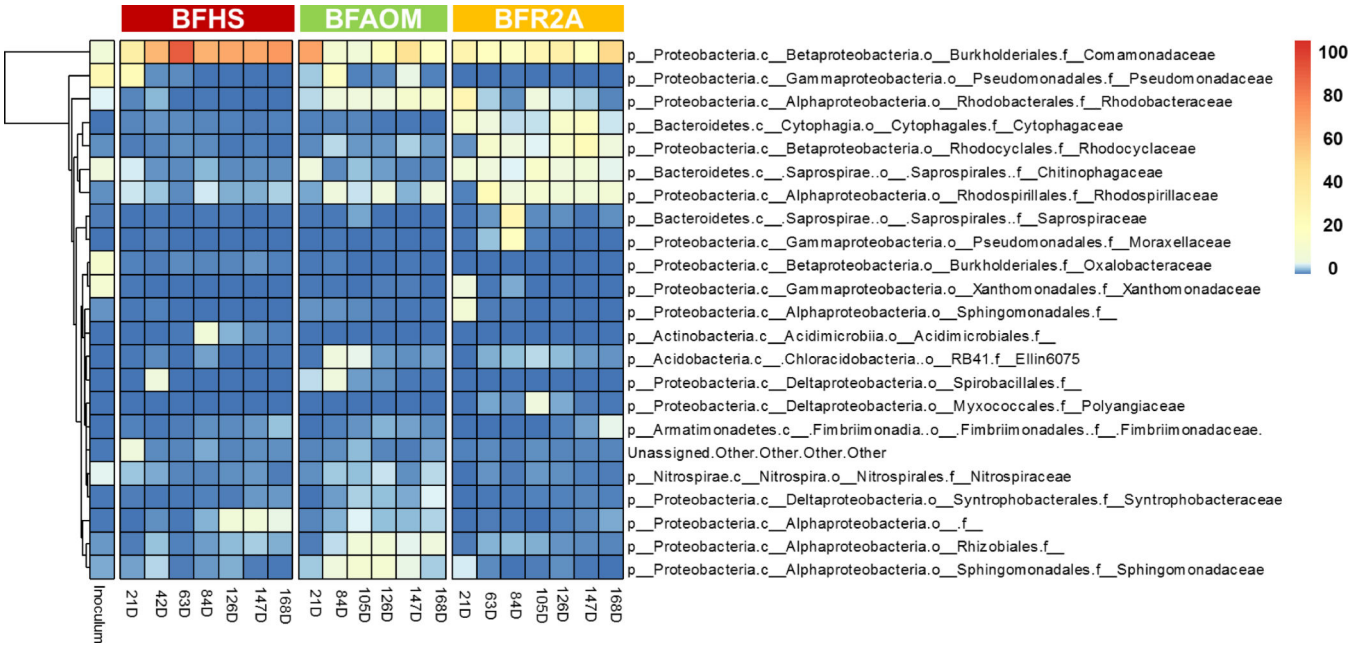

Fig. 6.

The relative distribution of bacterial community compositions at the family level (present at a relative abundance > 4%) in the inoculum, BFHS, BFAOM, and BFR2A samples. For each biofilm sample, the DNA extracts from two biofilm grown-coupons were used for sequencing.

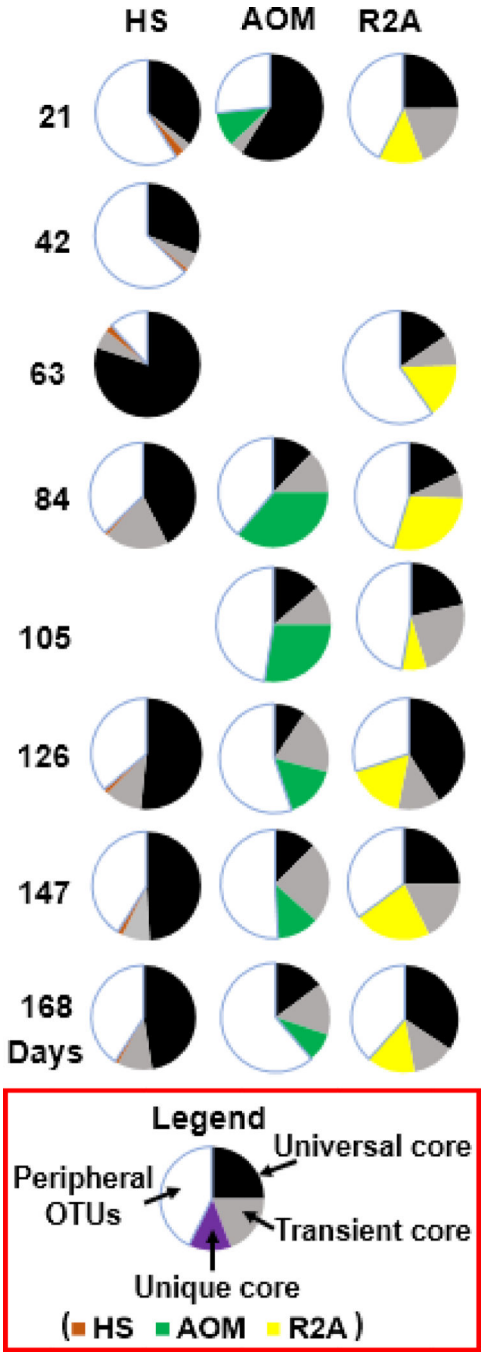

Fig. 7.

The dynamics of relative abundance of core OTUs (universal core, transient core, unique core) and peripheral OTUs for BFHS, BFAOM, and BFR2A samples. For each biofilm sample, the DNA extracts from two biofilm grown-coupons were used for sequencing. The four blank spots correspond to lost samples.

Table 1

Water chemistry parameters and EEM-PARAFAC components (organic matter compositions) of three different bulk water categories: HS, AOM, and R2A-impacted bulk water.

	HS reactor		AOM reactor		R2A reactor		
	Mean	**SD***	**Mean**	**SD**	**Mean**	**SD**	
Turbidity (NTU)	1.54	0.23	0.83	0.21	0.15	0.02	**Water quality parameters**
pH	7.80	0.08	7.82	0.04	7.38	0.03	
PO_4^{3-}(mg/L)	1.14	0.13	1.21	0.25	1.09	0.08	
AOC (μg/L)	137.27	9.29	139.27	12.25	140.37	16.23	
TOC (mg/L)	1.50	0.21	1.50	0.18	1.50	0.12	
TN (mg/L)	1.42	0.37	2.08	0.11	2.51	0.22	
TOC/TN	1.10	0.21	0.78	0.13	0.60	0.11	
$SUVA_{254}$ (L/mg C-m)	2.17	0.31	1.09	0.34	0.57	0.04	
Tyrosine-like materials (%)	6.46	1.49	6.38	1.43	28.12	1.51	**EEM-PARAFAC components**
SMP-like materials (%)	7.36	1.42	12.10	2.21	29.15	2.01	
Tryptophan-like materials (%)	13.32	2.29	26.68	3.79	28.65	2.40	
LMW humic-like substances (%)	32.14	4.58	28.02	1.54	9.81	1.23	
HMW humic-like substances (%)	40.72	3.89	26.82	2.27	4.27	0.92	

*represents standard deviation